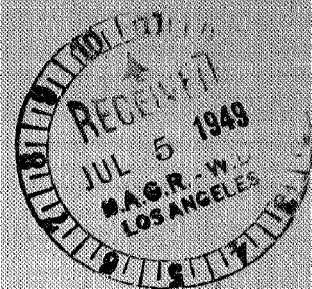


NACA TN 1907

# NATIONAL ADVISORY COMMITTEE FOR AERONAUTICS

TECHNICAL NOTE 1907



AN ANALYSIS OF THE TRANSITION OF A HELICOPTER FROM  
HOVERING TO STEADY AUTOROTATIVE VERTICAL DESCENT

By A. A. Nikolsky and Edward Seckel

Princeton University

TECHNICAL LIBRARY  
AIRESEARCH MANUFACTURING CO.  
9851-9951 SEPULVEDA BLVD.  
INGLEWOOD,  
CALIFORNIA



Washington  
June 1949



NATIONAL ADVISORY COMMITTEE FOR AERONAUTICS

---

TECHNICAL NOTE 1907

---

AN ANALYSIS OF THE TRANSITION OF A HELICOPTER FROM  
HOVERING TO STEADY AUTOROTATIVE VERTICAL DESCENT

By A. A. Nikolsky and Edward Seckel

SUMMARY

An analytical study is presented of the transition from hovering flight (power on) to steady vertical descent (in autorotation) following power failure while hovering. The effects of hinging the blades, of blade moment of inertia, and of rapidity of pitch reduction after power failure are investigated.

The results indicate that the effect of blade flapping is negligible as far as the establishment of steady autorotation is concerned. From the standpoint of avoiding excessive blade stalling during the transition, it is desirable that the blade pitch be reduced as rapidly as possible after power failure, and that the blade moment of inertia be large.

Sample calculations and graphs of computed transitions for a typical helicopter are presented.

INTRODUCTION

This report is the second phase of a broad program of study of the transient motions of helicopters in autorotative flight. The first phase (reference 1) dealt with the steady-state condition of autorotative vertical descent. This report is concerned with the transition from the steady condition of hovering to the steady autorotative descent.

It has long been realized that the ability of a helicopter to establish steady autorotation following power failure would be an important safety feature. Although some helicopters have successfully demonstrated such an ability, there has been no analytical method available for assessing the influence of the design variables on the ease and safety of performing such a maneuver.

Such a method, based on numerical integration of the equations of motion, is presented in this report.

Validity of the analysis presented here is limited to cases where blade stalling can be neglected throughout the maneuver, and therefore where the rotor is in no danger of stopping. Nevertheless the investigation is sufficient to indicate the effects of certain important variables.

This work was conducted at Princeton University under the sponsorship and with the financial assistance of the National Advisory Committee for Aeronautics.

### SYMBOLS

#### Physical Quantities

W	gross weight of helicopter, pounds
b	number of blades per rotor
R	blade radius, feet
r	radial distance to blade element, feet
c	blade-section chord, feet
$c_e$	equivalent blade chord, feet $\left( c_e = \frac{\int_0^R cr^2 dr}{\int_0^R r^2 dr} \right)$
$\sigma$	rotor solidity ratio $\left( \frac{bc_e}{\pi R} \right)$
$\theta$	blade-section pitch angle from zero lift, radians unless otherwise stated
$I_1$	mass moment of inertia of blade about flapping hinge, slug-feet <sup>2</sup>
$\rho$	mass density of air, slugs per cubic foot
t	time, seconds
g	acceleration of gravity (32.2 ft/sec <sup>2</sup> )

## Velocities

$V$	true airspeed of helicopter along flight path, feet per second
$V_v$	vertical component of $V$ (positive down, as in descent)
$\Omega$	rotor angular velocity, radians per second
$v$	induced velocity at rotor (always positive), feet per second
$\lambda$	inflow ratio (assuming $v$ constant over the disk) $\left( \frac{V_v - v}{\Omega R} \right)$

## Blade-Element Aerodynamic Characteristics

$c_{d_0}$	section profile-drag coefficient
$c_{d_0}'$	$c_{d_0}$ corrected for friction torque, auxiliary mechanisms, and so forth
$\delta_0, \delta_0', \delta_1, \delta_2$	coefficients in power series for $c_{d_0}$ as a function of angle of attack $\left( c_{d_0} = \delta_0 + \delta_1 \alpha_r + \delta_2 \alpha_r^2 \right)$ or $\left( c_{d_0}' = \delta_0' + \delta_1 \alpha_r + \delta_2 \alpha_r^2 \right)$
$\Delta c_{d_0}, \Delta \delta_0$	increment in $c_{d_0}$ to account for friction torque, and so forth $\left( \Delta c_{d_0} = c_{d_0}' - c_{d_0} = \Delta \delta_0 = \delta_0' - \delta_0 \right)$
$a$	slope of lift curve, per radian

## Rotor Aerodynamic Characteristics

T	rotor thrust, pounds
Q	rotor torque, pound-feet
$C_Q$	torque coefficient $\left( C_Q = \frac{Q}{\pi \rho R^3 (\Omega R)^2} \right)$

## Rotor-Blade Motion

$\beta$	flapping angle, radians unless otherwise noted
---------	--

## Miscellaneous

k	decay constant in assumed variation of induced velocity with time
$a_1, a_2, A_1, A_2$	constants in expression for $\theta$ as a function of time; $A_1$ and $A_2$ in radians unless otherwise noted
$b_1, b_2, b_3$	coefficients in differential equation for $\beta(t)$
$B_1, B_2, B_3, B_4, B_5, B_6, B_7$	coefficients in complete solution for $\beta(t)$ , radians unless otherwise noted
$m_1, \alpha, \omega$	decay constants in expression for $\beta(t)$
Subscripts:	
0	initial value, for hovering
f	final value, for steady autorotative vertical descent
a	average value $\left( ( )_a = \frac{1}{2} [( )_0 + ( )_f] \right)$
$\Delta t$	value after time interval of $\Delta t$ seconds

## ANALYSIS

It is assumed that the initial steady state of hovering flight is entirely determined, and the physical quantities of this hovering condition are denoted by the subscript 0. In the final state of steady autorotative descent, the subscript f is used to denote the physical quantities.

The simultaneous differential equations governing the transition period are six in number:

(1) For the vertical acceleration of the craft, with the rotor thrust a function of  $\Omega$ ,  $V$ ,  $v$ ,  $\beta$ ,  $\dot{\beta}$ ,  $\theta$ , and so forth.

(2) For the angular acceleration of the rotor, with the rotor torque a function of  $\Omega$ ,  $V$ ,  $v$ , and so forth.

(3) For the flapping motion of the blades.

(4) For the hunting motion of the blades.

(5) For the induced velocity  $v$  as a function of  $T$ ,  $V$ ,  $\dot{V}$ , and so forth (unsteady flow).

(6) For the angle of incidence  $\theta$  as a function of the flapping and lag angles.

There is as yet neither theory nor empirical data on which to base the fifth of the above equations. For convenience, it is assumed that the induced velocity  $v$  varies with time after power failure according to

$$v = v_f + (v_0 - v_f)e^{-kt} \quad (1)$$

where the value of the decay coefficient  $k$  is arbitrary and may be assigned different values in order to investigate its importance. It may be anticipated that the effect of the approximation represented by equation (1) is small, and that the value of  $k$  chosen is not critical, when the initial and final values of induced velocity are not widely different, as in the usual case. The induced velocity is considered to be constant over the rotor disk. While exponential variation of induced velocity (equation (1)) represents a convenient assumption, it is not unlikely that the actual variation would be somewhat different. Verification of the supposition that the effect is small, must, failing a theoretical approach, await experimental evidence.

It is assumed that the angle of incidence varies with time exponentially, and according to

$$\theta = \theta_f + A_1 e^{-a_1 t} + A_2 e^{-a_2 t} \quad (2)$$

where  $A_1$ ,  $A_2$ ,  $a_1$ , and  $a_2$  are arbitrary, except that

$$A_1 + A_2 = \theta_0 - \theta_f \quad (2a)$$

The changes in incidence due to flapping or hunting are thus combined with whatever changes the pilot may make manually. By suitably choosing the constants,  $A_1$ ,  $A_2$ ,  $a_1$ , and  $a_2$ , rapid or slow pitch reductions after power failure may be investigated. Thus, the necessity of solving the fourth, fifth, and sixth of the basic equations is obviated, by the assumptions represented by equations (1) and (2), and the problem simplified enormously.

It may further be anticipated that the variation of  $\beta$  with time will be of minor importance both to the designer and in its effect on the variations of  $V$  and  $\Omega$  with time. For the analysis of flapping angle it is therefore assumed that, in the transient period,  $\Omega$  is a constant and has the value of the average between  $\Omega_0$  and  $\Omega_f$ . This average value is denoted by  $\Omega_a$ .

In the following analysis only untwisted and untapered blades are considered. The equations developed on this basis can probably be applied to any blades, with fair accuracy, by using "equivalent" chord and angle of incidence.

#### Solution for $\beta$

The equation for the vertical acceleration of the helicopter may then be written as

$$V = g - \frac{\rho b a c R^3 \Omega_a^2}{2 \frac{W}{g}} \left( \frac{V - v}{2 \Omega_a R} - \frac{\dot{\beta}}{3 \Omega_a} + \frac{\theta}{3} \right) \quad (3)$$

and the equation for the transient flapping motion is

$$I_1(\beta \Omega_a^2 + \ddot{\beta}) = \frac{\rho a c R^4 \Omega_a^2}{2} \left( \frac{V - v}{3 \Omega_a R} - \frac{\dot{\beta}}{4 \Omega_a} + \frac{\theta}{4} \right) \quad (4)$$

Solving equation (4) for  $V$ , differentiating for  $\dot{V}$ , and substituting in equation (3) gives

$$\ddot{\beta} + b_1 \dot{\beta} + b_2 \beta + b_3 \beta = b_4 + \frac{\rho a c R^3 \Omega_a}{6 I_1} \left( -v + \frac{3}{4} \Omega_a R \dot{\theta} + \frac{\rho a b c R^3 \Omega_a^2}{48 W/g} \theta \right) \quad (5)$$

where

$$b_1 = \frac{\rho a c R^3 \Omega_a}{2 I_1} \left( \frac{R}{4} + \frac{b I_1}{2 R W/g} \right)$$

$$b_2 = \frac{\rho a c R^3 \Omega_a}{6 I_1} \left( \Omega_a^2 + \frac{\rho a b c R^3 \Omega_a}{48 W/g} \right)$$

$$b_3 = \frac{\rho a b c R^2 \Omega_a^3}{4 W/g}$$

$$b_4 = \frac{g \rho a c R^3 \Omega_a}{6 I_1}$$

The transient solution of equation (5) is of the form

$$\beta = B_1 e^{m_1 t} + e^{\alpha t} (B_2 \cos \omega t + B_3 \sin \omega t) \quad (6)$$



where the roots of

$$m^3 + b_1 m^2 + b_2 m + b_3 = 0 \quad (7)$$

are

$$\left. \begin{aligned} m &= m_1 \\ m &= \alpha \pm j\omega \end{aligned} \right\} \quad (7a)$$

where

$$j = \sqrt{-1}$$

The steady-state solutions have the same form as the forcing functions, and together must satisfy equation (5). Thus the steady-state solutions are:

$$\beta = B_4 + B_5 e^{-kt} + B_6 e^{-a_1 t} + B_7 e^{-a_2 t} \quad (8)$$

where, by substitution into equation (5) and equating coefficients of identical terms,

$$B_4 = \beta_f \quad (8a)$$

$$B_5 = \left( \frac{\rho a c R^3 \Omega_a}{6I_1} \right) \frac{k(v_f - v_0)}{(k^3 - b_1 k^2 + b_2 k - b_3)} \quad (8b)$$

$$B_6 = \left( \frac{\rho a c R^3 \Omega_a}{6I_1} \right) \left( \frac{\frac{3}{4} \Omega_a R A_1 a_1 - \frac{\rho a b c R^3 \Omega_a^2}{48W/g} A_1}{a_1^3 - b_1 a_1^2 + b_2 a_1 - b_3} \right) \quad (8c)$$

$$B_7 = \left( \frac{\rho a c R^3 \Omega_a}{6 I_1} \right) \left( \frac{\frac{3}{4} \Omega_a R A_2 a_2 - \frac{\rho a b c R^3 \Omega_a^2}{48 W/g} A_2}{a_2^3 - b_1 a_2^2 + b_2 a_2 - b_3} \right) \quad (8d)$$

The initial conditions, which must be satisfied by the complete solution for  $\beta(t)$ , are that, at  $t = 0$ ,

$$\beta = \beta_0 \quad (9)$$

$$\dot{\beta} = \dot{\beta}_0 = 0 \quad (9a)$$

$$\ddot{\beta} = \ddot{\beta}_0 = \frac{\rho a c R^4 \Omega_0^2}{2 I_1} \left( \frac{V_0 - v_0}{3 \Omega_0 R} + \frac{\theta_0}{4} \right) - \beta_0 \Omega_0^2 \quad (9b)$$

Therefore, from equations (9),

$$B_1 + B_2 + B_4 + B_5 + B_6 + B_7 = \beta_0 \quad (10)$$

$$m_1 B_1 + \alpha B_2 + \omega B_3 - k B_5 - a_1 B_6 - a_2 B_7 = 0 \quad (10a)$$

$$m_1^2 B_1 + (\alpha^2 - \omega^2) B_2 + 2\omega\alpha B_3 + k^2 B_5 + a_1^2 B_6 + a_2^2 B_7 = \ddot{\beta}_0 \quad (10b)$$

Equations (10), (10a), and (10b) can be solved for  $B_1$ ,  $B_2$ , and  $B_3$ , when  $B_4$  through  $B_7$  have been found by equations (8). The complete solution, then, is

$$\begin{aligned} \beta(t) = & B_1 e^{m_1 t} + e^{\alpha t} (B_2 \cos \omega t + B_3 \sin \omega t) + \\ & B_4 + B_5 e^{-kt} + B_6 e^{-a_1 t} + B_7 e^{-a_2 t} \end{aligned} \quad (11)$$

Solution for  $\Omega$  and  $V$ 

The remaining two variables are  $V(t)$  and  $\Omega(t)$ . The equations to be solved are the thrust and torque equations:

$$\dot{V} = g - \frac{\rho a b c R^3}{2W/g} \left( \frac{V - v}{2R} \Omega - \frac{\dot{\beta}}{3} \Omega + \frac{\theta^2}{3} \Omega^2 \right) \quad (12)$$

and

$$\dot{\Omega} = \frac{\rho c R^4 \Omega^2}{2I_1} \left[ \frac{\lambda^2 f_1}{2} - \frac{\lambda}{3} (f_3 - f_1 f_2) - \frac{f_2 f_3 + \delta_0'}{4} \right] + \frac{2\beta \dot{\beta} \Omega}{I_1} \quad (13)$$

where

$$f_1 = a - \delta_2$$

$$f_2 = \theta - \dot{\beta}/\Omega$$

$$f_3 = a \dot{\beta}/\Omega + \delta_1 + f_2 \delta_2$$

and  $\beta(t)$  is known approximately from equation (11).

Equations (12) and (13) can be solved by a tabular, step-by-step process as outlined below.

A sample calculation has been performed (fig. 1), by the step-by-step process, comparing the results obtained by including and neglecting the  $\dot{\beta}$  terms in equations (12) and (13). Reference to the figure will show that the effect of flapping is negligible on the variations of  $\Omega(t)$



and  $V(t)$ . The flapping terms are therefore neglected in the following development of the step-by-step method of solving equations (12) and (13). In effect, then, only rigid blades are considered, although the effects of blade flapping would be negligible.

Equations (12) and (13) then become

$$\dot{V} = g - \frac{\rho abc R^3}{2W/g} \left( \frac{V - v}{2R} \Omega + \frac{\theta}{3} \Omega^2 \right) \quad (12a)$$

and

$$\ddot{\Omega} = \frac{\rho c R^4}{2I_1} \left[ \frac{a - \delta_2}{2R^2} (V - v)^2 - \frac{\delta_1 - \theta(a - 2\delta_2)}{3R} \Omega (V - v) - \frac{\delta_0' + \delta_1\theta + \delta_2\theta^2}{4} \Omega^2 \right] \quad (13a)$$

By differentiating equation (13a),

$$\ddot{\Omega} = \frac{\rho c R^4}{2I_1} \left\{ \frac{(a - \delta_2)}{R^2} (V - v)(\dot{V} - \dot{v}) - \frac{\delta_1 - \theta(a - \delta_2)}{3R} [\Omega(\dot{V} - \dot{v}) + \dot{\Omega}(V - v)] + \frac{\dot{\theta}(a - 2\delta_2)}{3R} \Omega (V - v) - \frac{\delta_0' + \delta_1\theta + \delta_2\theta^2}{2} \Omega \dot{\Omega} - \frac{\dot{\theta}}{4} (\delta_1 + 2\theta\delta_2) \Omega^2 \right\}$$

At zero time (the instant of power failure) all the quantities in the above equations (12a), (13a), and (14) are known. The step-by-step process is started by computing from these the values of  $\dot{V}_0$ ,  $\dot{\Omega}_0$ , and  $\ddot{\Omega}_0$ . After a short interval of time, say  $\Delta t$  seconds, the new value of rotor angular velocity  $\Omega_{\Delta t}$  may be found approximately from the abbreviated Taylor series:

$$\Omega_{\Delta t} = \Omega_0 + (\Delta t)\dot{\Omega}_0 + \frac{(\Delta t)^2}{2}\ddot{\Omega}_0 \quad (15)$$

It is assumed that the change in  $V$  in the period  $\Delta t$  is the time  $\Delta t$  times the average rate of change of  $V$  in the time interval  $\Delta t$ . Thus,

$$V_{\Delta t} = V_0 + \frac{\Delta t}{2}(\dot{V}_0 + \dot{V}_{\Delta t}) \quad (16)$$

From equation (12a),

$$\dot{V}_{\Delta t} = g - \frac{\rho abc R^3}{2W/g} \left[ \frac{\dot{\Omega}_{\Delta t}}{2R} (V_{\Delta t} - v_{\Delta t}) + \frac{\theta \Delta t}{3} \Omega_{\Delta t}^2 \right] \quad (17)$$

Solving equations (16) and (17) simultaneously for  $\dot{V}_{\Delta t}$  (the unknowns being  $\dot{V}_{\Delta t}$  and  $V_{\Delta t}$ ),

$$\dot{V}_{\Delta t} = \frac{g - \frac{\rho abc R^3}{2W/g} \left[ \frac{\dot{\Omega}_{\Delta t}}{2R} \left( V_0 + \frac{\Delta t}{2} \dot{V}_0 - v_{\Delta t} \right) + \frac{\theta \Delta t}{3} \Omega_{\Delta t}^2 \right]}{1 + \Delta t \frac{\rho abc R^2}{8W/g} \Omega_{\Delta t}} \quad (18)$$

whence  $V_{\Delta t}$  may be found from equation (16).

Now  $\dot{\Omega}_{\Delta t}$  may be computed from equation (13a) and the approximate value of  $\Omega_{\Delta t}$  from equation (15) checked by

$$\Omega_{\Delta t} = \Omega_0 + \frac{\Delta t}{2}(\dot{\Omega}_0 + \dot{\Omega}_{\Delta t}) \quad (19)$$

If this does not check quite closely the value first obtained from equation (15), and used in equation (18), a trial-and-error process can be used to find  $\Omega_{\Delta t}$ . In this case, a value of  $\Omega_{\Delta t}$  would be assumed, in place of equation (15), used in equation (18), and then checked by equation (19). Good agreement should be achieved before the process is repeated for the next interval. Experience has shown that for  $\Delta t = \frac{1}{2}$  second, the first estimate furnished by equation (15) is usually checked quite closely (within 0.05 radian/sec) by equation (19).

This process is repeated for as many intervals of time as are necessary for  $\Omega$  and  $V$  to reach their final steady values in steady autorotation.

A running check can be kept on the approach to the instability caused by excessive blade stalling (see reference 1) by computing the value of the inflow ratio  $\lambda$  at every interval of time, and spotting  $\lambda$  and  $\theta$  on curves of  $Q$  against  $\lambda$  and  $\theta$ , in which the effect of blade stall has been included, as in figure 3 of reference 1. The value of  $\lambda$  is given by

$$\lambda = \frac{(V - v)}{\Omega R} \quad (20)$$

Long before the "second, unstable trim point" (described in reference 1) is approached, however, it would be necessary to use modified equations (12a) and (13a), altered to include the effects of blade stalling. In this case, the trick represented by equation (15) to improve the convergence of the step-by-step process would be excessively complex to apply. The trial-and-error process necessary to carry out the numerical integration of the new equations (12a) and (13a) would be arduous at each interval of time, and, for adequate accuracy, the time intervals would have to be much more frequent.



## A SAMPLE DESIGN STUDIED

Using the methods described in the preceding section, the transitions from hovering to steady autorotation have been computed for a helicopter with the following physical characteristics:

$$\begin{aligned} W &= 2700 \text{ pounds} & c &= 1.25 \text{ feet} \\ b &= 3 & a &= 5.6 \text{ per radian} \\ R &= 20 \text{ feet} & c_{d_0}' &= 0.0087 - 0.0216\alpha_r + 0.400\alpha_r^2 \\ I_1 &= 100, 200, 400 \text{ slug-feet}^2 \end{aligned}$$

This sample design is the same as was considered in reference 1, for which the steady autorotative characteristics were computed.

The initial hovering state considered is

$$\begin{aligned} V_0 &= 0 & v_0 &= 21.25 \text{ feet per second} \\ \Omega_0 &= 25.1 \text{ radians per second} & \theta_0 &= 7.25^\circ = 0.1265 \text{ radian} \end{aligned}$$

For transitions in which the pitch is reduced after power failure, the final state considered is

$$\begin{aligned} V_f &= 31.2 \text{ feet per second} & v_f &= 25.1 \text{ feet per second} \\ \Omega_f &= 20.8 \text{ radians per second} & \theta_f &= 4^\circ = 0.0698 \text{ radian} \end{aligned}$$

For transitions in which the pitch is not reduced, the final steady state is taken as

$$\begin{aligned} V_f &= 30.5 \text{ feet per second} & v_f &= 26.4 \text{ feet per second} \\ \Omega_f &= 16.5 \text{ radians per second} & \theta_f &= 7.25^\circ = 0.1265 \text{ radian} \end{aligned}$$

The various ways in which the pitch is changed, for this investigation, are illustrated in figure 2. The different curves correspond to different values of the constants  $A_1$ ,  $A_2$ ,  $a_1$ , and  $a_2$  (equation (2)).

The variations of induced velocity with time, given by equation (1), are illustrated in figure 3, for  $k = 1$ , and, in the cases of pitch reduction after power failure, for  $k = \infty$ .

## RESULTS AND DISCUSSION

### Probable Effect of Assuming the Variation of

#### Induced Velocity with Time

A typical variation of descending velocity  $V$  and rotor angular velocity  $\Omega$  with time after power failure is illustrated in figure 4. These calculations were made by the step-by-step process given in the section entitled "Solution for  $\Omega$  and  $V$ ," neglecting flapping. Two calculations were made, for  $k = 1.0$  and  $\infty$ , in order to evaluate the importance of  $k$ .

Since, in the usual case, the initial and final values for the induced velocity are not very different, it seems intuitively evident that the exact variation of  $v(t)$  ought not to affect the variations of  $V(t)$  and  $\Omega(t)$  appreciably. This is confirmed by figure 4, where  $V(t)$  and  $\Omega(t)$  are compared for the widely different values of  $k$ , representing the variations of  $v(t)$  shown in figure 3.

It may be observed that, if the induced velocity varied in such a manner that its value was not always between the initial and final values, then it might be important to consider the actual variation. In that case,  $v(t)$  would have to be determined from experiment. It should be remarked that, in the solution for  $\Omega(t)$  and  $V(t)$  just referred to, any suitable variation of  $v(t)$  may be assumed. The exponential variation was convenient in the analytical solution for  $\beta(t)$ .

### Interpretation of the Different Rates of Pitch

#### Change Considered

The extremes of the types of pitch change considered are the uppermost and lowermost curves of figure 2, representing no pitch change and instantaneous pitch reduction at the instant of power failure. The case of no pitch change could occur with rigid blades (or hinged blades so

articulated that a change in lag angle would not change the incidence) if the pilot failed to alter the pitch manually. The instantaneous pitch change could be approached by a rotor having articulated blades with no damping about the drag hinge. In this case, the change in lag angle would be very rapid, and any attendant change of incidence could be considered practically instantaneous. The intermediate, exponential types of pitch change could each occur, for articulated blades, with an infinite number of combinations of pilot reaction and degrees of damping about the drag hinge. The more gradual changes are associated with slower pilot reaction and greater damping about the drag hinge. For rigid blades, the curves represent only different pilot reactions.

#### Variations of Flapping Angle $\beta$ with Time After

##### Power Failure

The influence of the different rates of pitch change, and of blade moment of inertia, on the variation of flapping angle  $\beta$  with time is given in figure 5. These calculations were made by the method of equation (11), using the induced-velocity decay coefficient  $k$  equal to unity.

The variations of  $\beta(t)$  shown in figure 5 are of passing interest only, since the effects of blade flapping are of no importance in the variations of  $V(t)$  and  $\Omega(t)$ . In spite of the linearizing assumption in the solution for  $\beta(t)$  that  $\Omega$  is constant, figure 5 probably gives a good indication of stop-settings required on the flapping hinge to allow the blades complete freedom in this maneuver. The final values of  $\beta$  are different for the case of no pitch change and the cases of pitch reduction because the final values of  $\Omega$  are not the same.

#### Effect of Blade Flapping on $V(t)$ and $\Omega(t)$

Comparison (fig. 1) of two computations of  $V(t)$  and  $\Omega(t)$ , for instantaneous pitch change, shows that the effect of blade flapping is negligible. The case of instantaneous pitch change was chosen for this comparison, since the variations of  $\beta$  are greatest for this case (fig. 5). If the flapping hinge is so directed that a change in  $\beta$  causes a change in incidence, then in equation (2) for  $\theta(t)$  the influence of flapping must be considered. The value of  $k$  was taken to be unity.



## Influence of Rate of Pitch Reduction and Blade

### Moment of Inertia on $V(t)$ and $\Omega(t)$

The influence of rate of pitch change and blade moment of inertia on the variation of flapping angle with time is shown in figure 5; the effect of blade moment of inertia on  $V(t)$  and  $\Omega(t)$  is shown in figure 6. It may be considered that the average time required to effect the transition for the cases considered is about 6 seconds. With regard to avoiding the instability caused by blade stalling at high values of  $\lambda$  (see the study of stability of autorotation, reference 1), it is desirable to keep  $\lambda$  to a minimum throughout the maneuver.

In order to evaluate the effects of rate of pitch reduction and moment of inertia in this regard, figures 7 and 8 are presented. The solid lines represent boundaries determined from reference 1, figure 3. For any value of  $\theta$ , the point on the boundary was determined by the value of  $\lambda$  at which the difference in  $\frac{2C_Q}{\sigma}$  due to neglecting blade stalling was 0.0015. Thus the boundaries shown indicate, for any value of  $\theta$ , an arbitrary limit for  $\lambda$ , above which blade stalling should be accounted for in equations (12a) and (13a). The broken curves are the loci of combinations of  $\lambda$  and  $\theta$  computed during the maneuvers considered in the study of the sample design. As can be seen from the figures, all the cases computed lie within the range of  $\lambda$  and  $\theta$  where blade stalling can be neglected, as has been done in the ANALYSIS.

From figure 7, the advantage of a rapid pitch reduction is apparent, for keeping  $\lambda$  to a minimum throughout the maneuver, and hence in avoiding the instability of excessive blade stalling. From figure 8, a similar advantage for large blade moment of inertia is to be noted.

For larger initial blade angles in hovering than considered here, the maneuver can only be investigated by accounting for blade stalling, and then only with grave reservations because of the assumption of constant induced velocity, which assumption was shown in reference 1 to be severe in cases where blade stalling is important. It can, however, be anticipated that, in this case, the importance of rapid rate of pitch reduction and large blade moment of inertia would be greatly magnified.

### Descending Velocity against Altitude Lost

Figures 9 and 10 show descending velocity against altitude lost during the maneuvers investigated. Altitude lost is obtained by graphical integration of the curves of  $V(t)$ , figures 5 and 6. The

average drop required to effect the transition, for the cases considered, is seen to be about 120 feet.

The effect of rate of pitch change on descending velocity at a given amount of altitude lost, from figure 9, is apparently small. This conclusion is obviously limited to cases where the hovering incidence is within the range for steady autorotation. If  $\theta_0$  were greater than the maximum for steady autorotation (reference 1, fig. 3), then obviously the pitch would have to be reduced rapidly to avoid the instability caused by excessive blade stalling.

From figure 10, the advantage of a large blade moment of inertia, in preserving a minimum descending velocity for a given altitude lost, is readily apparent.

### CONCLUSIONS

Analytical methods are given for treating the transient motion of a helicopter between the hovering state and the steady autorotative state of vertical descent. From the standpoint of avoiding blade stalling in the transition, it is desirable to reduce pitch rapidly and to have a large blade moment of inertia.

The effects of hinging the blades, for a given net rate of pitch reduction after power failure, appear to be negligible.

The average time to effect the transition from hovering to steady autorotation is about 6 seconds, for the cases investigated. The corresponding average altitude lost in the transition is about 120 feet.

Princeton University

Princeton, N. J., May 12, 1948

## REFERENCE

1. Nikolsky, A. A., and Seckel, Edward: An Analytical Study of the Steady Vertical Descent in Autorotation of Single-Rotor Helicopters. NACA TN 1906, 1949.

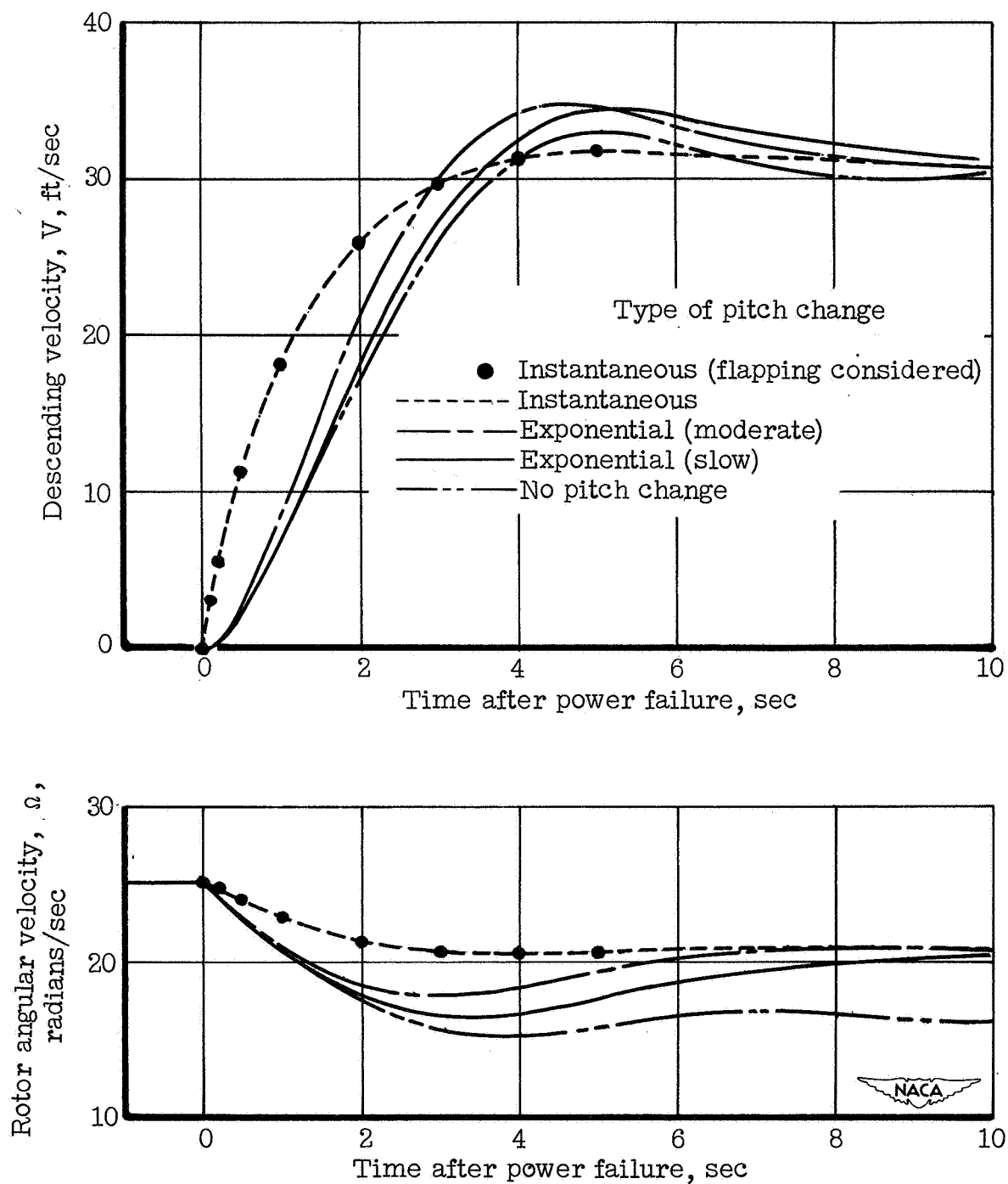


Figure 1.- Effect of rate of pitch reduction on the variations of descending velocity and rotor angular velocity with time after power failure. Flapping neglected except as noted.  $I_1 = 200$  slug-feet<sup>2</sup>.

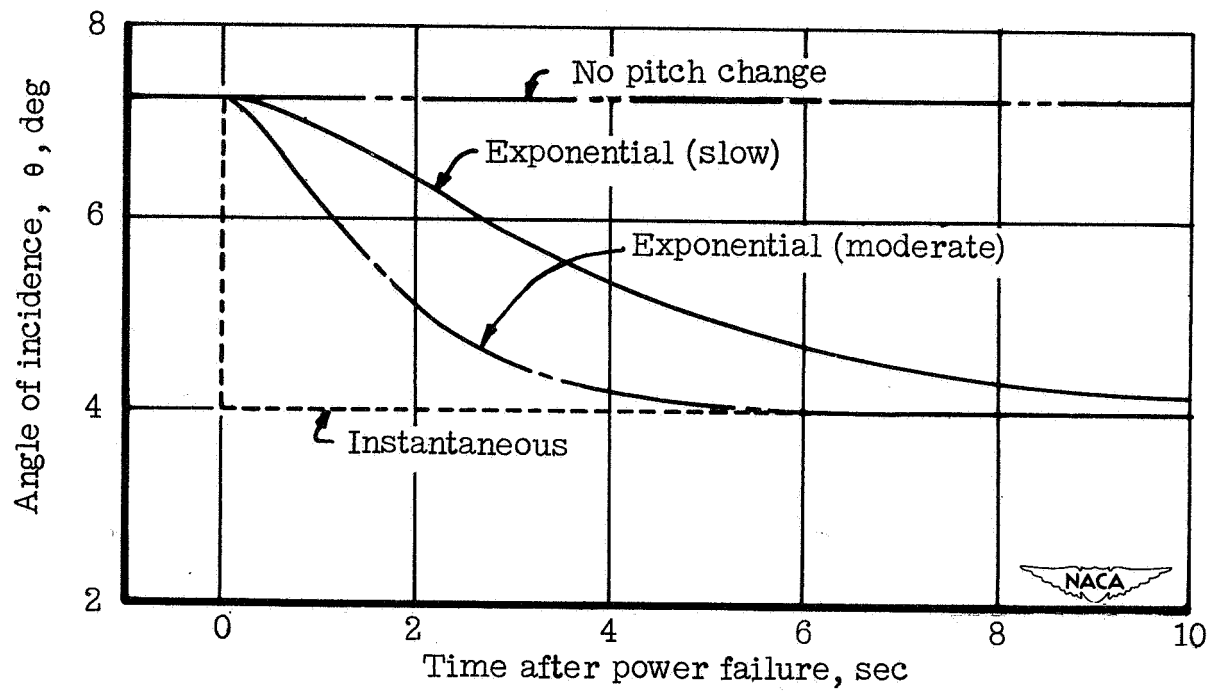


Figure 2.- Types of pitch change considered.



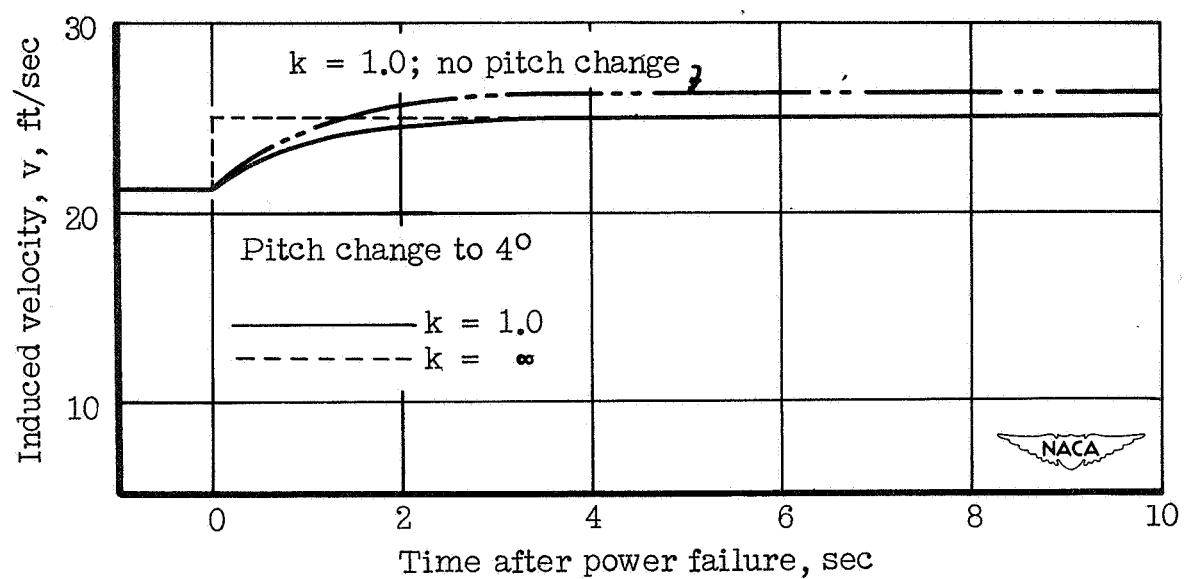


Figure 3.- Assumed variations of induced velocity with time after power failure.

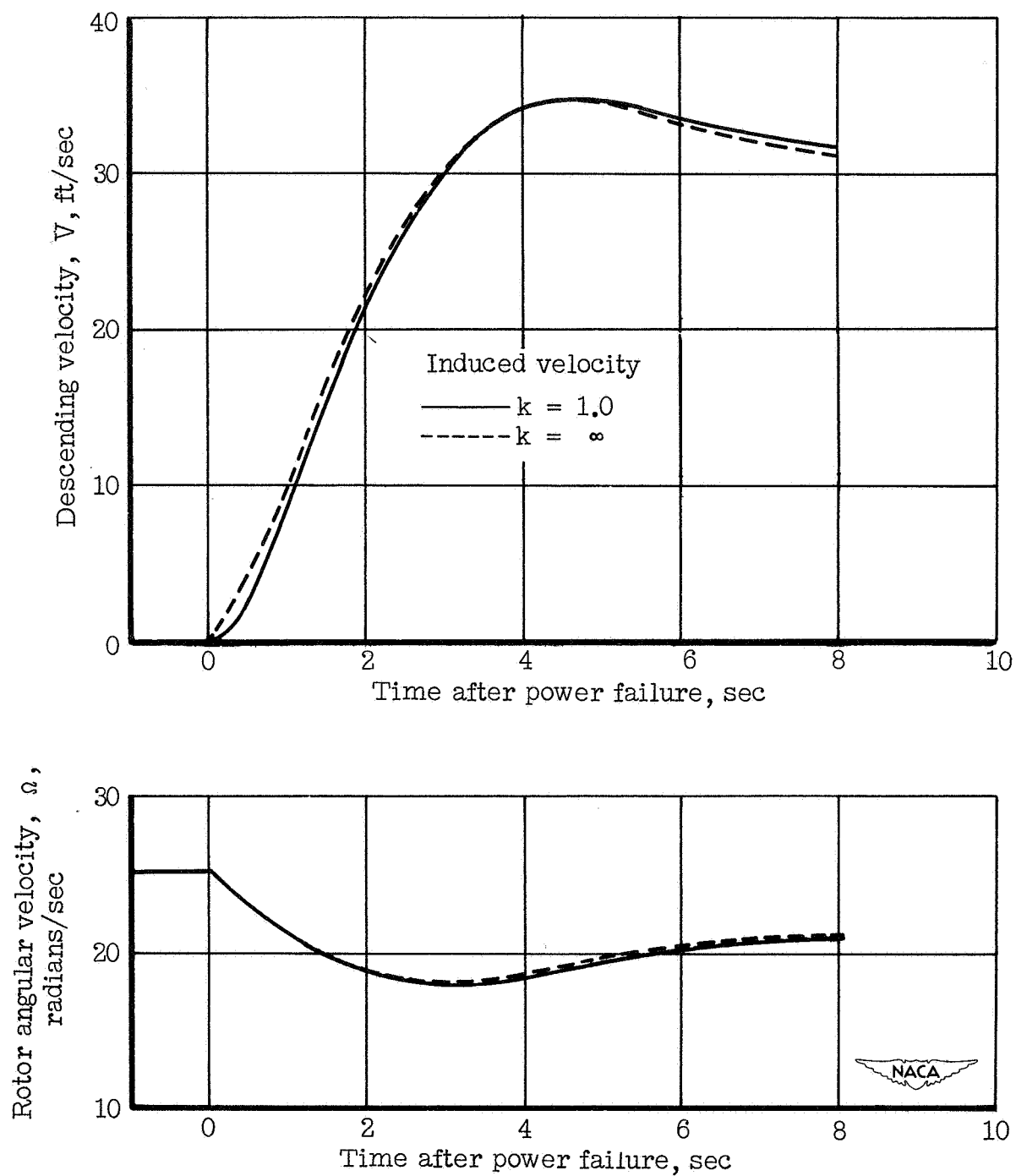


Figure 4.- Effect of two different assumptions for induced velocity against time on the variations of descending velocity and rotor angular velocity with time after power failure.  $v = v_f + (v_0 - v_f)e^{-kt}$ . (See fig. 3.)

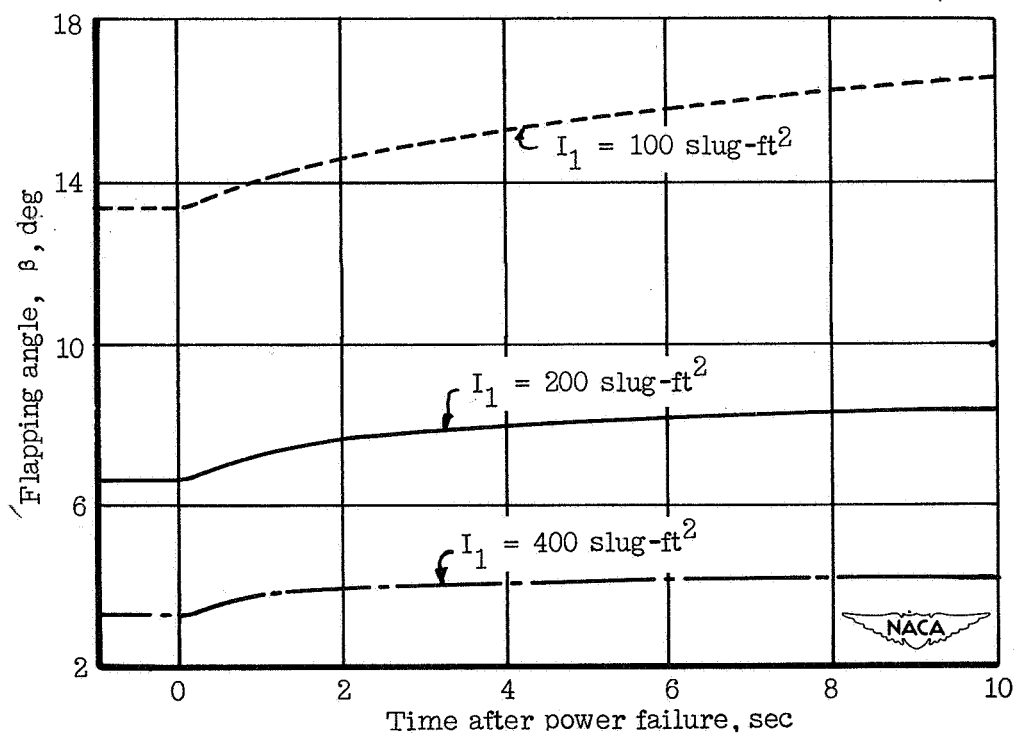
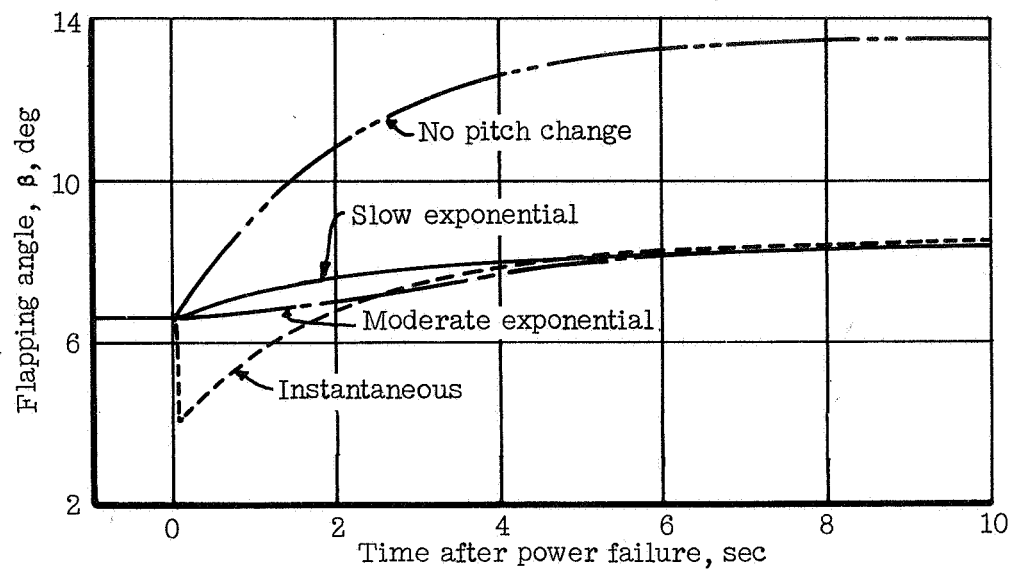


Figure 5.- Effects of rate of pitch reduction and blade moment of inertia on the variation of flapping angle with time after power failure.

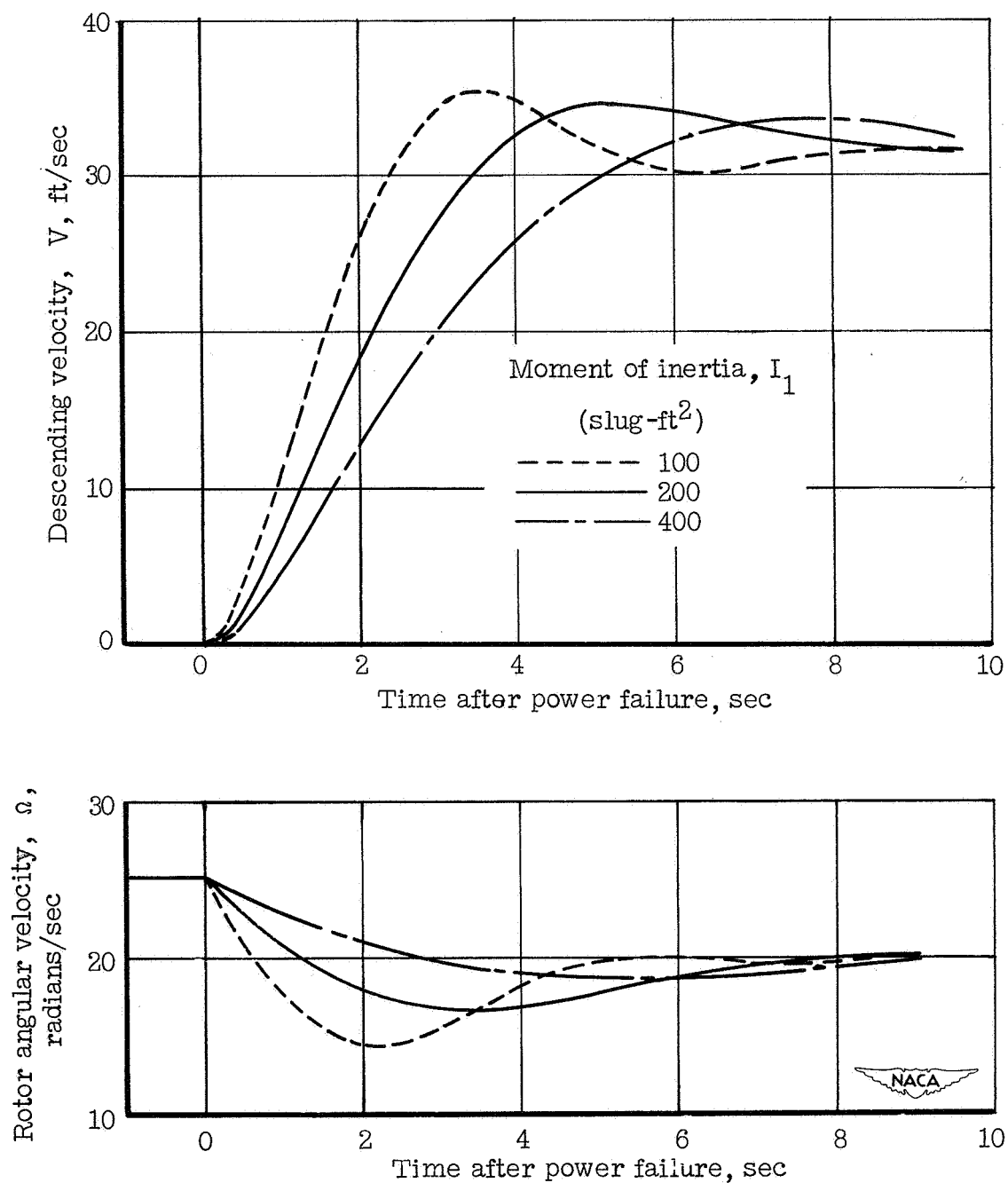


Figure 6.- Effect of blade moment of inertia on the variations of descending velocity and rotor angular velocity with time after power failure. Slow exponential pitch change (fig. 2).

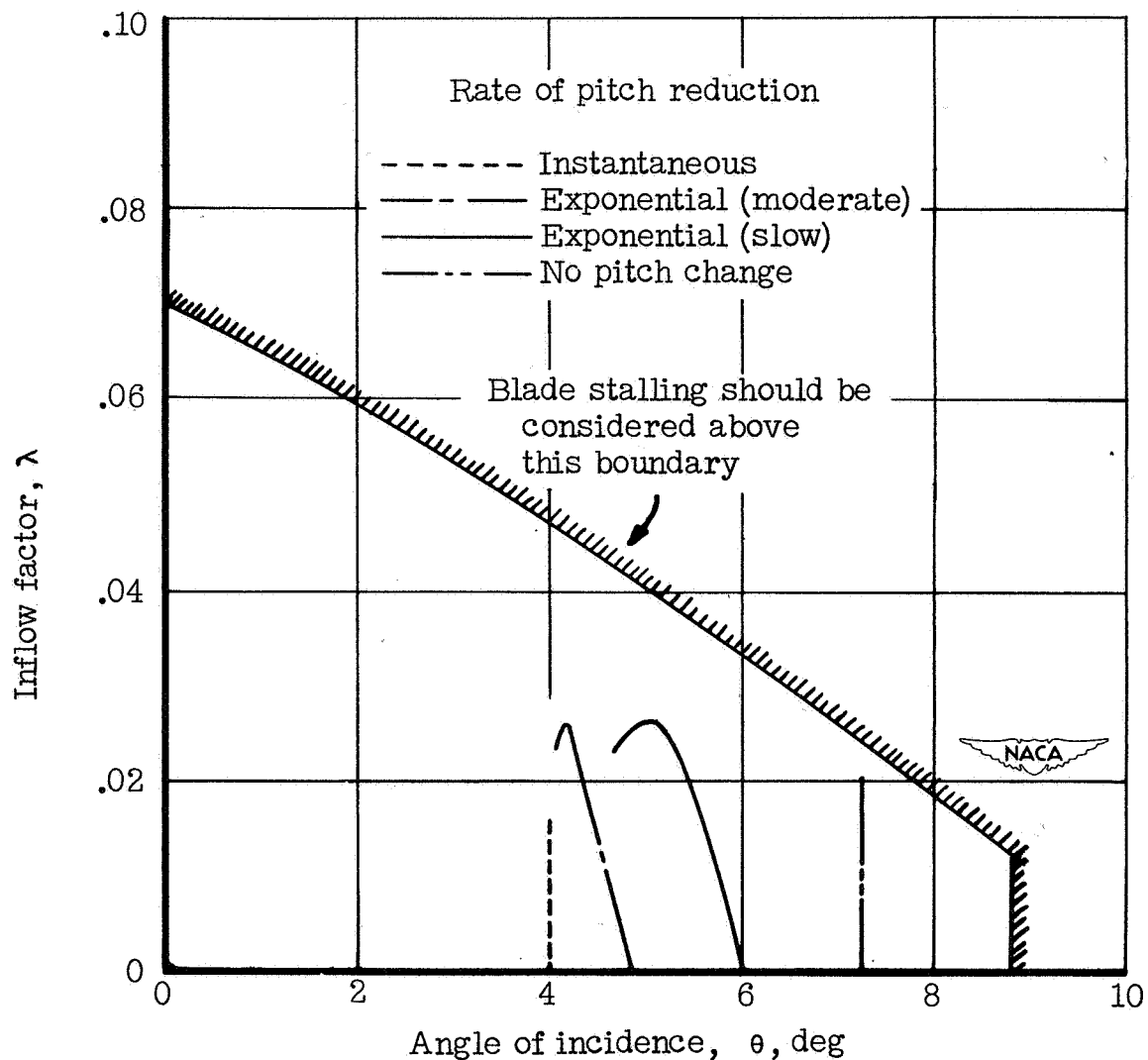


Figure 7.- Effect of rate of pitch reduction on  $\lambda$  against  $\theta$  throughout the transition maneuver.  $I_1 = 200$  slug-feet<sup>2</sup>.



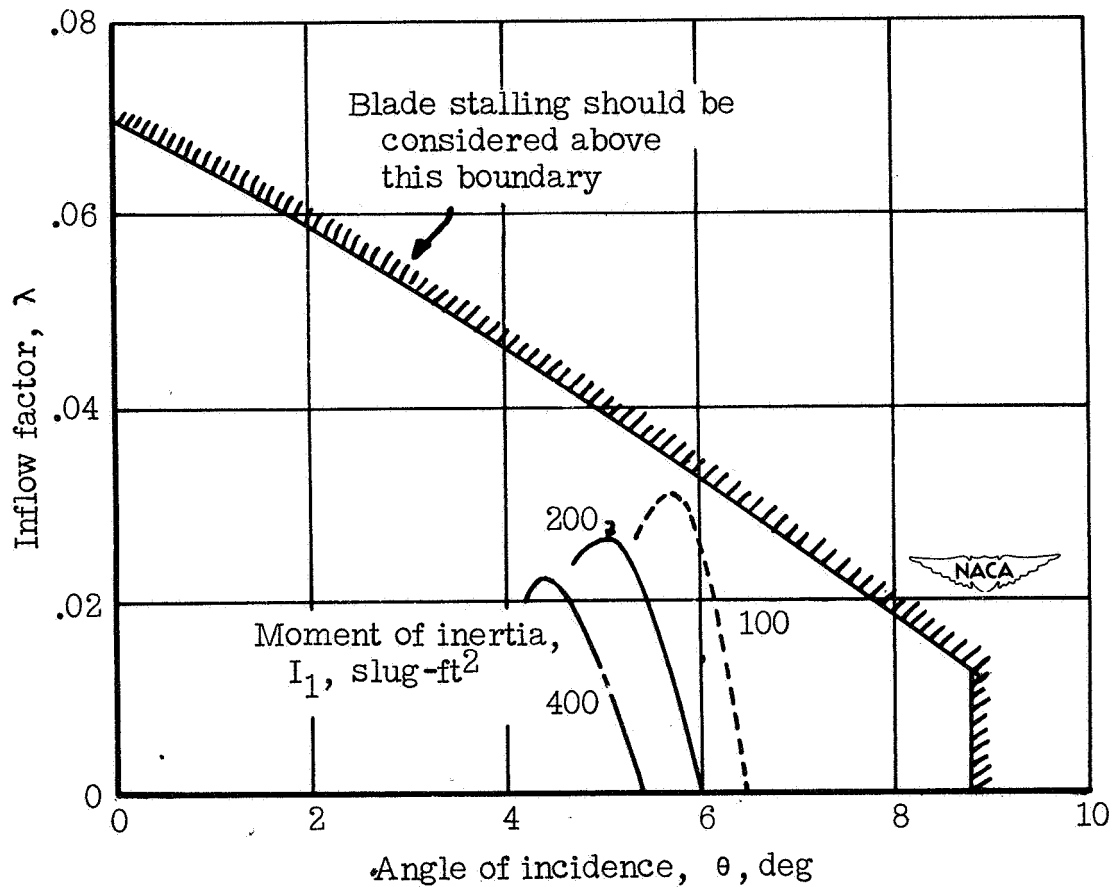


Figure 8.- Effect of blade moment of inertia on  $\lambda$  against  $\theta$  throughout the transition maneuver. Slow exponential pitch change.

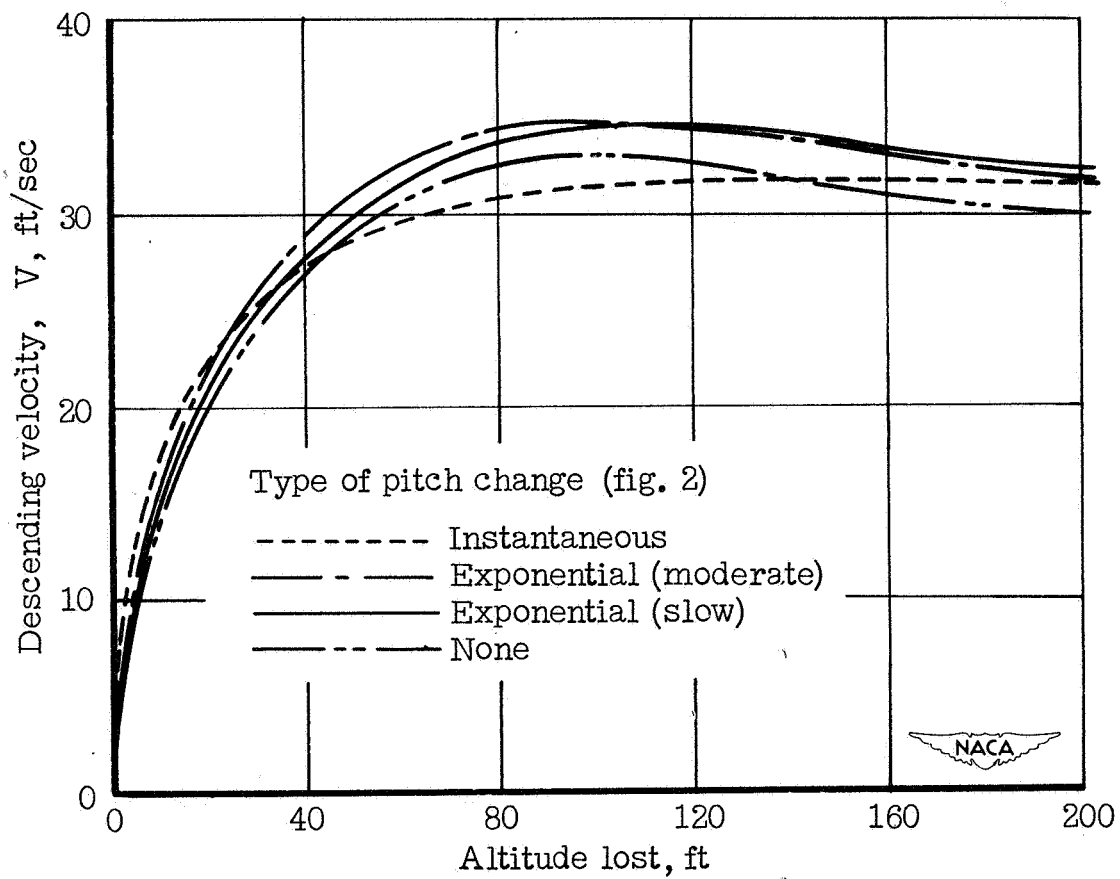


Figure 9.- Effect of rate of pitch reduction on descending velocity against altitude lost.  $I_1 = 200$  slug-feet<sup>2</sup>.

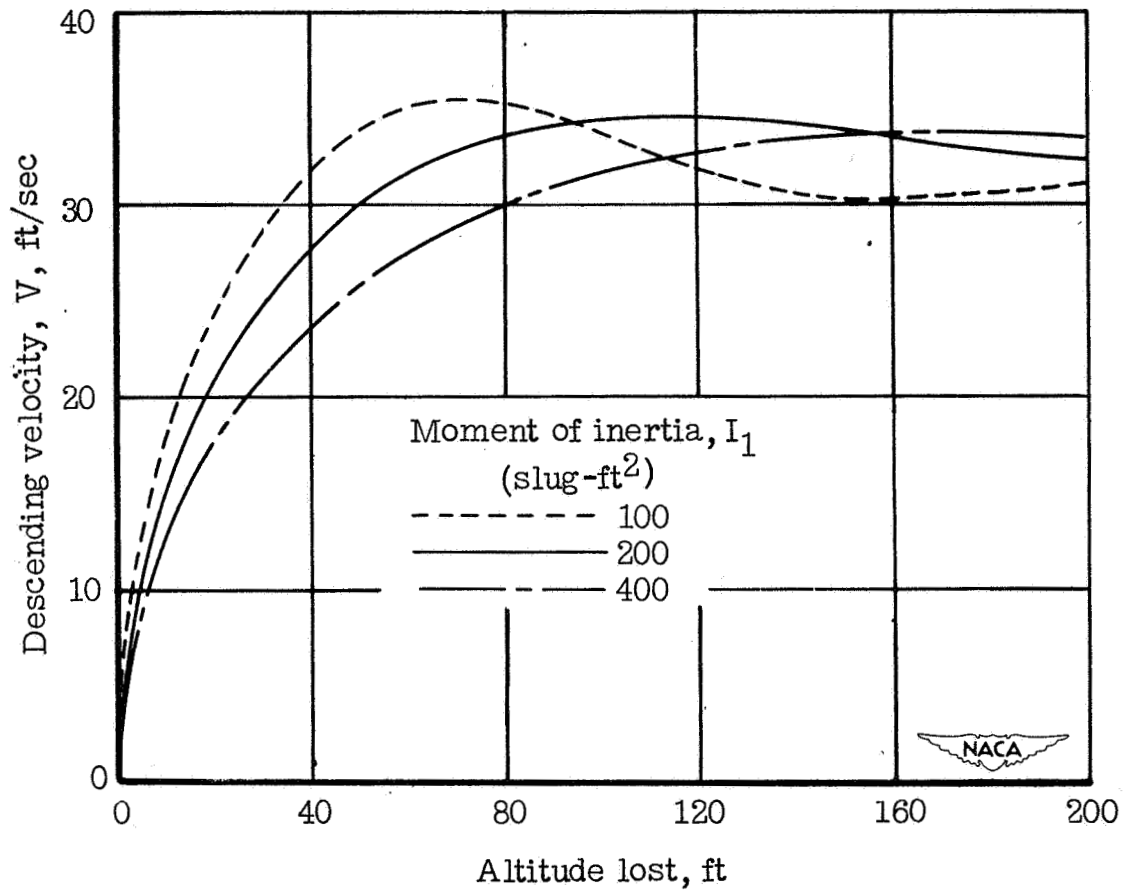


Figure 10.- Effect of blade moment of inertia on descending velocity against altitude lost. Slow exponential pitch change.